Inorganic Chemistry
Article
Cite This: Inorg. Chem. XXXX, XXX, XXX−XXX
pubs.acs.org/IC

A Thiol-Functionalized UiO-67-Type Porous Single Crystal: Filling in the Synthetic Gap

Yan-Lung Wong,[†] Yingxue Diao,[‡] Jun He,[§] Matthias Zeller,[⊥] and Zhengtao Xu*[,†]

[†]Department of Chemistry and [‡]Department of Materials Science and Engineering, City University of Hong Kong, 83 Tat Chee Avenue, Kowloon, Hong Kong, China

[§]School of Chemical Engineering and Light Industry, Guangdong University of Technology, Guangzhou 510006, Guangdong, China

[⊥]Department of Chemistry, Purdue University, 560 Oval Drive, West Lafayette, Indiana 47907, United States

Supporting Information

ABSTRACT: Thiol groups (−SH) offer versatile reactivity for functionalizing metal−organic frameworks, and yet thiol-equipped MOF solids remain underexplored due to synthetic challenges. Building on the recent breakthrough using benzyl mercaptan as the sulfur source and $AlCl_3$ for uncovering the thiol function, we report on the thiol-equipped linker 3,3′-dimercaptobiphenyl-4,4′-dicarboxylic acid and its reaction with Zr(IV) ions to form a UiO-67-type MOF solid with distinct functionalities. The thiol-equipped UiO-67 scaffold shows substantial stability toward oxidation, e.g., it can be treated with 30% H_2O_2 to afford oxidation of the thiol to the strongly acidic sulfonic function while maintaining the ordered porous MOF structure. The thiol groups also effectively take up palladium(II) ions from solutions to allow for comparative studies on catalytic activities and to help elucidate how the spatial configuration of the thiol groups can be engineered to impact the performance of heterogeneous catalysis in the solid state. Comparative studies on the stability in the solventless (activated) state also help to highlight the steric factor in stabilizing UiO-67-type frameworks.

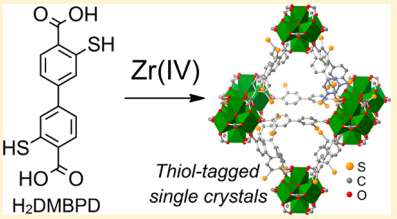

INTRODUCTION

The combination of carboxyl with phenol[1−3] or thiophenol[4−13] units offers intriguing opportunities for constructing metal−organic frameworks. For example, the DOBD ligand[14] and metal ions form the MOF-74 solids[15] (H_2DOBD = 2,5-dihydroxybenzene-1,4-dicarboxylic acid, Figure 1) featuring

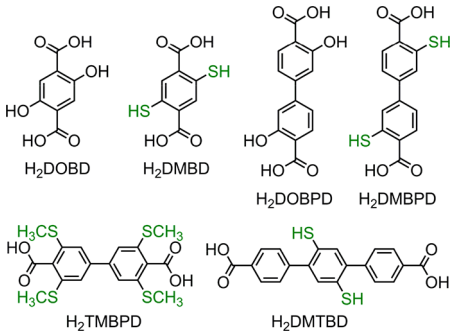

Figure 1. Six linear dicarboxyl aromatics equipped with hydroxyl or sulfur functions.

simultaneously phenol and carboxyl-metal coordination, offering robust frameworks with open metal site functions.[16−18] Its rod packing motif also obviates interpenetration to yield large-aperture networks.[19] Additionally, the metal-phenoxide bonds promotes interactions between metal centers and organic π-systems and enables solid-state electronic and electrocatalytic properties.[20−22] Such electronic properties are further highlighted in the DMBD-based frameworks (H_2DMBD: 2,6-dimercaptanbenzene-1,4-dicarboxylic acid), wherein Mn or Fe-DMBD solids, as the sulfur analogs of MOF-74, exhibit enhanced charge transport behaviors.[23,24] Moreover, the softer sulfur groups (e.g., in H_2DMBD) readily allow the carboxyl groups to bond selectively with hard metal centers such as Zr(IV), Al(III), and Cr(III), to create MOF solids with highly tailorable free-standing thiol functions.[4−7,10−12] The harder phenol group (e.g., in H_2DOBD), by comparison, is more prone to bond to hard metal centers, even though a few hydroxyl-equipped Zr-MOF solids with free-standing OH functions are also known.[1,25−27] In a wider perspective, the modularity of MOF synthesis[28,29] naturally applies here to include the extended linker DOBPD (dobpdc^{4-}: 4,4′-dioxidobiphenyl-3,3′-dicarboxylate, Figure 1)[30,31] and even longer linker systems[19] for achieving larger-pore features.

By contrast, the thiol counterparts remain scarce, as if the modularity game were suddenly lost on the community. The real challenge, however, lies in the lack of efficient, wide-scope synthetic methods for thiol-equipped carboxyl linker molecules. For example, synthesis of the thiol-equipped acid molecule H_2DMBPD, as the thiol analog of the increasingly known H_2DOBPD, has not been reported (even though the sulfonate analog, prepared by a sulfonation-oxidation protocol, was recently reported).[32] The recent development of a thiol-carboxyl linker synthesis[7] is therefore important for the systematic exploration of thiol-equipped MOF solids. We

Received: October 23, 2018

DOI: 10.1021/acs.inorgchem.8b03000
Inorg. Chem. XXXX, XXX, XXX−XXX

here utilize this synthetic advance to bear on the simple yet unexplored molecule H_2DMBPD. In particular, we will describe a Zr(IV)-based single crystal system Zr-DMBPD [or UiO-67-$(SH)_2$], isoreticular to the UiO-67 prototype, i.e., Zr-BPD with fcc-arrayed Zr_6O_8 units,[33] but functionalized with well-defined, free-standing thiol arrays. Moreover, UiO-67-$(SH)_2$ also provides insights into the stability issue when compared with the relatively delicate UiO-67 solid and the very robust Zr-TMBPD crystal [UiO-67-$(SCH_3)_4$ (see Figure 1 for TMBPD]),[34] by highlighting the steric origin of the stability of the latter. We will also describe the catalytic activity of Pd-loaded crystals of UiO-67-$(SH)_2$ in comparison with the reported system of Zr-DMTBD [UiO-68-$(SH)_2$ (see Figure 1 for DMTBD]),[6] as an effort to engineer the spatial configuration of thiol arrays for modifying materials properties.

EXPERIMENTAL SECTION

The general procedures (including details of single-crystal X-ray diffraction data collection) are included in the Supporting Information.

Synthesis of Dimethyl 3,3′-Bis(fluoro)biphenyl-*p*,*p*′-dicarboxylate (SM1). Into a two-necked, round-bottomed flask containing a magnetic stirring bar, nickel(II) dichloride hexahydrate (2.034 g, 8.58 mmol), and PPh_3 (9.0 g, 34.3 mmol) on a nitrogen manifold was cannulated deaerated DMF (81 mL; bubbled with N_2 for 15 min). The mixture was then stirred to afford a deep blue solution, into which Zn powder (0.561 g, 8.58 mmol) was added under nitrogen protection. After heating at 50 °C for 1 h (with stirring; to give a red mixture), methyl 4-bromo-2-fluorobenzoate (2.0 g, 8.582 mmol) was added, and the reaction mixture was kept at 50 °C in N_2 atmosphere for another 6 h. After cooling to room temperature (rt), methyl iodide (2.2 mL, 35.34 mmol) was injected, and the resulting mixture was stirred for 2 h. The mixture was then poured into distilled water (300 mL), and the precipitate was collected by suction filtration, washed with distilled water (3 × 100 mL), redissolved in ethyl acetate (EA, 500 mL), dried over anhydrous $MgSO_4$, and purified by flash column chromatography (eluent: *n*-hexane/DCM from 1 to 0.5) to yield a white solid (920 mg, 70% based on methyl 4-bromo-2-fluorobenzoate). ^{1}H NMR (400 MHz, $CDCl_3$): δ = 8.02 (t, J = 7.8 Hz, 2H), 7.43 (dd, J = 8.2, 1.7 Hz, 2H), 7.36 (dd, J = 11.6, 1.6 Hz, 2H), 3.95 (s, 6H). ^{19}F NMR (376 MHz, $CDCl_3$): δ = −108.26 (s). ^{13}C NMR (100 MHz, $CDCl_3$) δ = 164.54 (d, J = 3.9 Hz), 163.57 (s), 160.98 (s), 144.97 (dd, J = 8.6, 1.8 Hz), 133.04 (d, J = 1.3 Hz), 122.68 (d, J = 3.6 Hz), 118.54 (d, J = 10.2 Hz), 115.84 (s), 115.60 (s), 52.59 (s). FT-IR (KBr pellet, ν/cm^{-1}): 1716 (s), 1620 (s), 1558 (m), 1439 (s), 1396 (s), 1311 (s), 1288 (s), 1254 (s), 1215 (m), 1192 (m), 1138 (s), 1107 (m), 1045 (w), 879 (w), 852 (w), 775 (m), 690 (w).

Synthesis of Dimethyl 3,3′-Bis(benzylthio)biphenyl-*p*,*p*′-dicarboxylate (SM2). Into a two-necked, round-bottomed flask containing a magnetic stirring bar, **SM1** (1.0 g, 3.26 mmol), and K_2CO_3 (3.16 g, 22.8 mmol) on a nitrogen manifold was cannulated deaerated *N*-methyl-2-pyrrolidone (NMP, 27 mL; bubbled with N_2 for 15 min), and stirring was started. Benzyl mercaptan (1.0 mL, 8.52 mmol) was added under N_2 protection, and the reaction mixture was stirred at 50 °C for 2 days. After cooling to rt, methyl iodide (1.0 mL, 16 mmol) was injected under N_2 protection and stirred for 1 h. The resulting mixture was then poured into distilled water (300 mL); 15 min later, the solid thereof was collected by suction filtration, washed with distilled water (3 × 100 mL), and dried in the air stream to afford **S7** as a white solid (1.64 g, 97.4% yield based on **SM1**). ^{1}H NMR (400 MHz, $CDCl_3$) δ = 7.74−7.68 (m, 2H), 7.36 (d, J = 1.7 Hz, 2H), 7.31 (d, J = 7.2 Hz, 4H), 7.22 (t, J = 7.3 Hz, 4H), 7.19−7.13 (m, 4H), 4.02 (s, 4H), 3.77 (s, 6H). ^{13}C NMR (100 MHz, $CDCl_3$) δ = 166.59 (s), 143.75 (s), 142.75 (s), 135.99 (s), 131.85 (s), 129.02 (s), 128.73 (s), 127.51 (s), 126.93 (s), 124.79 (s), 123.07 (s), 52.25 (s), 37.29 (s). FT-IR (KBr pellet, ν/cm^{-1}): 2951 (m), 1713 (s), 1589 (m), 4868 (m), 1493 (m), 1470 (m), 1454 (m), 1439 (m), 1281 (s), 1257 (s), 1242 (s), 1192 (m), 1161 (m), 1115 (s), 1057 (s), 771 (m), 729 (m), 706 (m).

Synthesis of Dimethyl 3,3′-Bis(acetylthio)biphenyl-*p*,*p*′-dicarboxylate (SM3). In a N_2-filled glovebox, anhydrous $AlCl_3$ (3.30 g, 24.8 mmol) and anhydrous toluene (41 mL) were added to a two-necked, round-bottomed flask charged with **SM2** (1.60 g, 3.11 mmol). The flask was then taken out of the glovebox and connected to a nitrogen manifold. After stirring at rt for 2 h, the mixture was chilled in an ice bath, and acetyl chloride (2.64 mL, 37 mmol) was injected under N_2 protection. The ice bath was removed, and the resulting mixture was stirred at rt for 1 h and then poured into an ice−water bath (200 mL) and extracted with DCM (3 × 100 mL). The combined organic layer was washed with distilled water (3 × 100 mL), dried over $MgSO_4$, evaporated in vacuo, and then subjected to flash column chromatography (eluent: *n*-hexane/DCM from 2 to 1) to yield a white solid (772 mg, 59.3% based on **SM2**). ^{1}H NMR (400 MHz, $CDCl_3$) δ = 8.04 (d, J = 8.1 Hz, 2H), 7.80 (d, J = 1.8 Hz, 2H), 7.69 (dd, J = 8.1, 1.9 Hz, 2H), 3.91 (s, 6H), 2.47 (s, 6H). ^{13}C NMR (100 MHz, $CDCl_3$) δ = 192.77 (s), 166.27 (s), 142.53 (s), 135.24 (s), 133.18 (s), 131.61 (s), 129.78 (s), 127.93 (s), 52.49 (s), 30.37 (s). FT-IR (KBr pellet, ν/cm^{-1}): 2958 (w), 2924 (w), 1720 (s), 1693 (s), 1593 (m), 1473 (w), 1450 (w), 1427 (w), 1358 (w), 1288 (s), 1265 (s), 1188 (w), 1122 (s), 1053 (m), 949 (w), 879 (w), 829 (w), 768 (w), 694 (w), 629 (m).

Synthesis of 3,3′-Bis(mercapto)biphenyl-*p*,*p*′-dicarboxylic Acid (H_2DMBPD). **SM3** (771 mg, 1.84 mmol) was placed in a two-necked, round-bottomed flask fitted with a septum and charged with a magnetic stirring bar. The flask was evacuated and refilled with N_2 3 times to afford N_2 protection, and a deaerated KOH solution (1.3 M, 28 mL in EtOH/H_2O, v/v = 1:1; bubbled by N_2 for 15 min) was then added via cannula. After being heated at 90 °C for 36 h, the reaction mixture was cooled to rt, and a deaerated HCl (10% in water, 16 mL; bubbled with N_2 for 5 min) was injected. The precipitate formed was filtered, washed extensively with deionized water, and dried on a filter paper under suction with a nitrogen steam to afford H_2DMBPD as a pale yellow solid (542 mg, 96% based on **SM3**). ^{1}H NMR (400 MHz, DMSO-d_6) δ = 8.02 (d, J = 8.2 Hz, 2H), 7.93 (d, J = 1.7 Hz, 2H), 7.53 (dd, J = 8.2, 1.7 Hz, 2H). ^{13}C NMR (100 MHz, DMSO-d_6) δ = 167.78 (s), 142.45 (s), 139.89 (s), 132.48 (s), 129.58 (s), 126.61 (s), 123.52 (s). FT-IR (KBr pellet, ν/cm^{-1}): 3063 (s), 2970 (s), 2870 (s), 2858 (s), 2654 (m), 2546 (m), 1678 (vs), 1593 (vs), 1554 (m), 1535 (m), 1500 (w), 1473 (m), 1419 (s), 1362 (m), 1311 (s), 1257 (vs), 1153 (m), 1061 (m), 922 (w), 876 (m), 833 (m), 810 (m), 771 (m). Chemical analysis of the product yielded the following: Calcd [C (54.89%), H (3.29%)]. Found [C (53.79%), H (3.27%)].

Preparation of UiO-67-$(SH)_2$ Single Crystals. Into a 25 mL Schlenk tube charged with H_2DMBPD (30 mg, 0.0979 mmol) was added *N*,*N*-diethylformamide (DEF, 1.1 mL) solution containing $ZrCl_4$ (22.8 mg, 0.0978 mmol) and benzoic acid (478 mg, 3.92 mmol). The tube was inserted into liquid N_2 to freeze the mixture and then evacuated in an oil pump vacuum. The tube was then screw-capped, naturally warmed to rt, and then heated at 120 °C in an oven for 24 h, followed by programmed cooling to rt over 12 h (at a rate of 7.9 °C h^{-1}). The resulting light yellow crystals were washed with DMF by decanting (5 × 3 mL) and then immersed in DMF for storage. For weighing, the crystals were solvent-exchanged with acetone (5 × 5 mL; over 10 min each time) and then dried in vacuo (yield 23.6 mg).

Bulk Synthesis of Polycrystalline UiO-67-$(SH)_2$ Sample. Into a 10 mL glass ampule charged with H_2DMBPD (120 mg, 0.39 mmol) was added a DEF (7.0 mL) solution containing $ZrCl_4$ (91.2 mg, 0.390 mmol) and benzoic acid (1.435 g, 11.75 mmol). The ampule was then evacuated by in oil pump vacuum (with the content being frozen in liquid nitrogen) and flame-sealed. The ampule was then naturally warmed to rt, heated at 120 °C in an oven for 24 h, and program-cooled back to rt over 12 h (at a rate of 7.9 °C h^{-1}). The solid product was washed with DMF (5 × 5 mL) and then stored in DMF. For weighing, the solid was solvent-exchanged with acetone (5 × 5 mL; over 10 min each time) and then dried in vacuo to give a light

DOI: 10.1021/acs.inorgchem.8b03000
Inorg. Chem. XXXX, XXX, XXX−XXX

yellow powder sample (153 mg, 73% based on $ZrCl_4$, see below for the composition of the as-made product). Elemental analyses found [C (32.56%), H (4.19%), N (0.44%)]. This analysis closely matches the formula $Zr_6O_4(OH)_4(DMBPD)_6(C_3H_7NO)(H_2O)_{35}$ (mw 3209), calcd: [C (32.56%), H (4.05%), N (0.44)].

Activation of UiO-67-$(SH)_2$. A thimble of folded filter paper containing an acetone-washed UiO-67-$(SH)_2$ crystalline sample (130 mg, dried under reduced pressure) was loaded into the main chamber of a Soxhlet extractor. The Soxhlet extractor was then mounted onto a 250 mL round-bottomed flask containing methanol (150 mL) and then equipped with a solvent condenser. After the solvent was heated in a 100 °C oil bath for 4 days, the filter paper was then taken out, and the solid was dried at 50 °C to afford the activated UiO-67-$(SH)_2$ sample. Removal of the DMF and DEF guests was manifested by elemental analysis, i.e., N content < 0.18%. The PXRD pattern of the activated sample indicated a single crystalline phase consistent with the as-made UiO-67-$(SH)_2$ sample.

Pd(II) Uptake by UiO-67-$(SH)_2$. An as-made sample of UiO-67-$(SH)_2$ (ca. 83 mg, stored in acetone) was solvent-exchanged with acetonitrile (3 × 5 mL). Afterward, the acetonitrile-covered sample (in 2 mL acetonitrile) was transferred using a glass dropper into a 100 mL round-bottomed flask containing an acetonitrile solution (60 mL) of $PdCl_2(CH_3CN)_2$ (400 mg). The flask was stoppered and heated at 70 °C for 1 day. After cooling to rt, the supernatant was decanted, and the resulted blood-red solid was soaked in fresh acetonitrile (10 mL) at 50 °C for 4 h. H_2S bubbling is useful for revealing Pd residue, which reacts with H_2S to turn the supernatant from colorless to pale yellow. The soaking step was repeated until the supernatant stays colorless throughout the H_2S test. After repeated washing, the resultant crystals were stored in acetonitrile to give UiO-67-$(SH)_2$-Pd. ICP analysis of a digested sample of UiO-67-$(SH)_2$-Pd indicated a Zr/Pd atom ratio of 1:0.42 (S/Pd ratio of 4.7), equivalent to a Pd content of 6.73 wt % (a higher loading of Pd was found difficult to achieve, even with longer soaking in an excess of a saturated acetonitrile solution of $PdCl_2$). To improve Pd loading, it may be helpful to conduct the MOF synthesis and solvent exchange with more rigorous exclusion of air, so as to fully prevent the oxidation of the −SH groups, e.g., oxidation that forms the less binding disulfide S−S bonds (see Figure S3 for the Raman spectra in which the humps around 480 cm^{-1} suggest the presence of S−S bonds).

Pd(II) Uptake by UiO-68-$(SH)_2$. A higher Pd loading of UiO-68-$(SH)_2$-Pd than that for UiO-67-$(SH)_2$ was achieved using a reported procedure.[6] In a clear glass vial, a sample of UiO-68-$(SH)_2$ (30 mg) was placed in an acetonitrile solution (7.0 mL) containing excess $Pd(CH_3CN)_2Cl_2$ (123 mg) at rt. The color of the crystals changed from light yellow to dark red immediately. After 12 h, the supernatant was decanted and the crystals were soaked in hot acetonitrile (about 70 °C, 10 mL × 3 each time, the crystals were allowed to soak for 3 h before the CH_3CN was decanted) to remove any residual unbound Pd(II) species. The soaking step was repeated until the supernatant stays colorless using the above-mentioned H_2S test. The obtained deep red crystals were dried in air to give the UiO-68-$(SH)_2$-Pd sample [37.8 mg, 93.1%, based on UiO-68-$(SH)_2$]. ICP analysis of a digested sample of UiO-68-$(SH)_2$-Pd indicated a Zr/Pd ratio of 1:0.7 (S/Pd ratio of 2.9) and a Pd content of 8.68 wt %.

For lower Pd loading into UiO-68-$(SH)_2$, a $PdCl_2$ solution of lower concentration and in smaller quantity (1.0 mL; 1000 ppm, cf 7200 ppm Pd in the above saturated solution) was used. An as-made sample of UiO-68-$(SH)_2$ (3 mg) was soaked in the solution at rt for 24 h. ICP analysis on the resulted sample finds an S/Pd atom ratio of 5.2, equivalent to a Pd content of 3.74 wt %. The UiO-68-$(SH)_2$-Pd crystals at this lower Pd loading are red, but not as dark as the above higher-loading sample.

Suzuki−Miyaura Reaction by UiO-67-$(SH)_2$-Pd. In open air atmosphere, iodobenzene (176 mg, 0.86 mmol), (4-(methoxycarbonyl)phenyl)boronic acid (220 mg, 1.22 mmol), and trimethylamine (165.1 mg, 1.63 mmol) were loaded in a 7.5 mL clear glass vial containing ethanol (3.0 mL). The UiO-67-$(SH)_2$-Pd solid catalyst (ca. 3.0 mg, S/Pd ratio of 4.7, Pd loading of 6.73%, ca. 1.9 × 10^{-3} mmol Pd) was then loaded to the solution. The mixture was stirred at 100 °C for 24 h, after which it was cooled back to rt and the crystals was separated from the supernatant by centrifugation. The crystalline solid was washed with DCM (3 × 5 mL), and the DCM solutions and the supernatant were combined and then washed with DI water (3 × 10 mL), dried over $MgSO_4$, and evaporated in vacuo. The obtained crude product was dissolved in $CDCl_3$ for ^1H NMR analysis to quantify the conversion rate of the product (methyl [1,1′-biphenyl]-4-carboxylate; using durene as an internal standard). The conversion of iodobenzene to methyl [1,1′-biphenyl]-4-carboxylate at 100 °C for 24 h was found to be 22.9% (TON for the single run: 104).

Suzuki−Miyaura Reaction by UiO-68-$(SH)_2$-Pd at Reported 2.9:1 S/Pd Ratio. In open air atmosphere, iodobenzene (166.5 mg, 0.816 mmol), (4-(methoxycarbonyl)phenyl)boronic acid (220.3 mg, 1.224 mmol), and triethylamine (165.1 mg, 1.632 mmol) were loaded in a 7.5 mL clear glass vial containing ethanol (3.0 mL). The UiO-68-$(SH)_2$-Pd crystals (ca. 1.0 mg, S/Pd ratio of 2.9, Pd loading of 8.68%, ca. 8.16 × 10^{-4} mmol Pd) were then added to the solution. The mixture was stirred and heated at 80 °C for 8 h, after which it was cooled back to rt and the catalyst separated from the supernatant by centrifugation. The crystalline solid was washed with DCM (3 × 5 mL), and the DCM solutions and the supernatant were combined and then washed with DI water (3 × 10 mL), dried over $MgSO_4$, and evaporated in vacuo. The obtained crude product was dissolved in $CDCl_3$ for ^1H NMR analysis to quantify the conversion rate of the product (methyl [1,1′-biphenyl]-4-carboxylate; using durene as the internal standard). The conversion of iodobenzene to methyl [1,1′-biphenyl]-4-carboxylate at 80 °C for 8 h was thus found to be 83.1% (TON for the single run: 831).

Suzuki−Miyaura Reaction by UiO-68-$(SH)_2$-Pd at 5.2:1 S/Pd Ratio. In open air atmosphere, iodobenzene (177 mg, 0.868 mmol), (4-(methoxycarbonyl)phenyl)boronic acid (220 mg, 1.22 mmol), and triethylamine (165 mg, 1.63 mmol) were loaded in a 7.5 mL clear glass vial containing ethanol (3.0 mL). The UiO-68-$(SH)_2$-Pd crystals (ca. 1.0 mg, S/Pd atom ratio of 5.2, Pd loading of 3.74%, ca. 3.51 × 10^{-4} mmol Pd) were then added to the solution. The mixture was stirred and heated at 80 °C for 8 h, after which it was cooled back to rt and the catalyst separated from the supernatant by centrifugation. The collected MOF catalyst was then washed with DCM (3 × 5 mL), and the combined organic layer was evaporated in vacuo. The obtained crude product was dissolved in $CDCl_3$ for ^1H NMR analysis to quantify the conversion rate of the product (methyl [1,1′-biphenyl]-4-carboxylate). The conversion of iodobenzene to methyl [1,1′-biphenyl]-4-carboxylate at 80 °C for 8 h was thus found to be 63.2% (TON for the single run: 1563).

Postsynthetic Oxidation of UiO-67-$(SH)_2$. In a 7.5 mL clear glass vial, an as-made sample of UiO-67-$(SH)_2$ (ca. 10 mg, stored in DMF) was solvent-exchanged with acetone (3 × 3 mL) and then water (3 × 3 mL) with over 10 min for each round of soaking. Afterward, the water supernatant was decanted and a solution of 30% H_2O_2 (aqueous, 1.0 mL) was added. The vial was then screw-capped and the mixture was gently stirred at rt for 1 day. The supernatant was decanted, and the solid was soaked in water (3 × 3 mL) and acetone (3 × 3 mL) for over 10 min each round. The resulting solid, denoted UiO-67-$(SO_3H)_2$, was then stored in acetone. Prior to IR and Raman measurements, this sample of UiO-67-$(SO_3H)_2$ was dried in oil pump vacuum for 6 h. However, this sample tends to gradually lose its crystallinity over a few days when exposed to air. For better PXRD characterization, the sample can be wetted by a small amount of DMF to minimize exposure to air during the data collection. After PXRD, the sample was washed with acetone (3 × 3 mL), dried in an oil pump vacuum for 4 h to be measured by solution ^1H NMR (solution prepared by dissolving the resultant crystal sample in 4% NaF in D_2O).

RESULTS AND DISCUSSION

Efficient Linker Synthesis. The synthesis builds on a recent synthetic advance[7] using benzyl mercaptan as a masked thiol agent that can be recovered by $AlCl_3$ (Figure 2). One

DOI: 10.1021/acs.inorgchem.8b03000
Inorg. Chem. XXXX, XXX, XXX−XXX

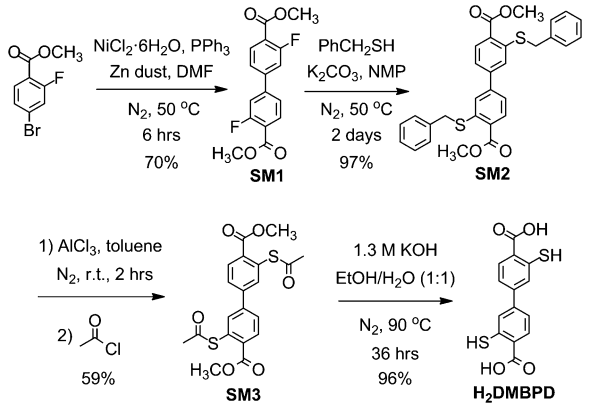

Figure 2. Synthesis of molecule H_2DMBPD.

hurdle to exploring thiol-equipped MOF solids is the synthesis of the organic linkers. For example, the thiol group can be derived from the phenol group via the Newman−Kwart rearrangement,[35−37] but this usually involves harsh high-temperature conditions, e.g., 200 °C; the lower-temperature protocols, e.g., enabled by Pd or photocatalysts,[38−40] remain to be tested in linker synthesis. Serious drawbacks also exist in reductive[41−43] and nucleophilic[44,45] dealkylation of thioethers, as these treatments are often incompatible with the donor groups, e.g., carboxyl, for MOF construction. The synthesis of H_2DMBPD serves to further showcase the recent advances in accessing carboxyl-thiol linkers for MOF construction. As shown in Figure 2, bis(fluoro)biphenyl diester **SM1** was obtained by a nickel-mediated homocoupling reaction;[46−49] aromatic nucleophilic substitution on **SM1** with benzyl mercaptan then formed dithioether compound **SM2** in an excellent yield (97%). The debenzylation step involved first stirring **SM2** in dry toluene with $AlCl_3$ and quenching with acetyl chloride to form stable dithioester **SM3**, which is suited for long-term storage and can be hydrolyzed to afford the linker H_2DMBPD on-demand.

Preparation and Characterization of MOF Solids. A solvothermal reaction of H_2DMBPD and $ZrCl_4$ in DEF (*N*,*N*-diethylformamide), with benzoic acid as the modulator and air excluded to minimize thiol oxidation, yielded single crystals of the framework ZrDMBPD, namely UiO-67-$(SH)_2$ [composition of an as-made sample: $Zr_6O_4(OH)_4(DMBPD)_6(C_3H_7NO)(H_2O)_{35}$, e.g., see also Figures S1−S3 for the TGA plot, IR, and Raman spectra]. Simple calculation indicates that the H_2O and DMF (C_3H_7NO) guests in this formula can be amply contained in the void space of the MOF solid (see the figure caption of Figure S1 for details). Like the prototype UiO-67 (based on 4,4′-biphenyl dicarboxylate)[33] and related UiO-67-type structures,[34,50] the X-ray crystal structure of UiO-67-$(SH)_2$ was solved in the space group $Fm\bar{3}m$ (No. 225; see also Table 1), consisting of a face-centered cubic array of $Zr_6O_4(OH)_4$ clusters bridged by the linear H_2DMBPD linkers to generate the fcu topology (see also Figure 3 for the porous architecture). The porosity of UiO-67-$(SH)_2$ was assessed by BET measurement using N_2 at 77 K. From the typical type-I gas adsorption isotherms, the corresponding surface area (S_{BET}) was determined to be 792 m^2/g (Figure S4), and the micropore volume (V_{micro}) was 0.363 $cm^3\ g^{-1}$. Both the measured surface area and pore volume of UiO-67-$(SH)_2$ are smaller than the values (S_{BET} = 1877 m^2/g and V_{micro} = 0.85 $cm^3\ g^{-1}$) reported for the unsubstituted UiO-67.[51] Analysis from the BET data indicated the pore diameter to be 8.52 Å (Figure S4), being consistent with the single crystal structure of UiO-67-$(SH)_2$.

Powder X-ray diffraction (PXRD) of solid samples of UiO-67-$(SH)_2$ indicated substantial long-term stability, even in the activated, solvent-free state. Specifically, the PXRD pattern of as-made UiO-67-$(SH)_2$ remains intact after staying in air for 5 days (Figure S5, cf. patterns b and d). The freshly activated sample also exhibits similarly sharp PXRD peaks (Figure 4, patterm c; or Figure S5, pattern e); Over an extended time period (e.g., 2 years), the diffraction peaks were found to be slightly broadened (Figure S5, pattern f), but these can all be indexed onto the original lattice of the UiO-67-$(SH)_2$ structure, indicating the retention of the host network. Even better stability had been reported in another UiO-67-type network [Zr-TMBPD, i.e., UiO-67-$(SCH_3)_4$; see Figure 1 for the structure of linker TMBPD], with the PXRD peaks of its

Table 1. Crystal Data and Structure Refinement Parameters for UiO-67-$(SH)_2$

compound	UiO-67-$(SH)_2$
chemical formula	$C_{84}H_{52}O_{37.55}S_{12}Zr_6$
formula weight	2594.09
temperature (°C)	−173
size (mm^3)	0.15 0.15 0.07
space group	$Fm\bar{3}m$
a, *b*, *c* (Å)	26.8367(4)
α, *β*, *γ* (deg)	90
V ($Å^3$)	19328.0(9)
Z	4
ρ_{calcd} (g/cm^3)	0.891
F(000)	5154
GOF	1.137
R_1 [$I > 2\sigma(I)$][a]	0.0572
wR_2 [$I > 2\sigma(I)$][b]	0.1774
CCDC number	1873767

[a] $R_1 = \sum||F_o| - |F_c||/\sum(|F_o|)$. [b] $wR_2 = \{\sum[w(F_o^2 - F_c^2)^2]/\sum[w(F_o^2)^2]\}^{1/2}$.

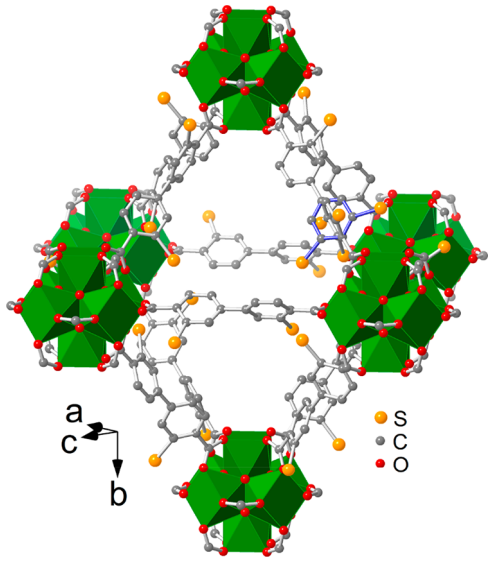

Figure 3. Octahedral cage from the single crystal structure of the UiO-67-$(SH)_2$ framework. The bluish purple benzene unit illustrates the disorder. Zr coordination polyhedra are displayed in green.

DOI: 10.1021/acs.inorgchem.8b03000
Inorg. Chem. XXXX, XXX, XXX−XXX

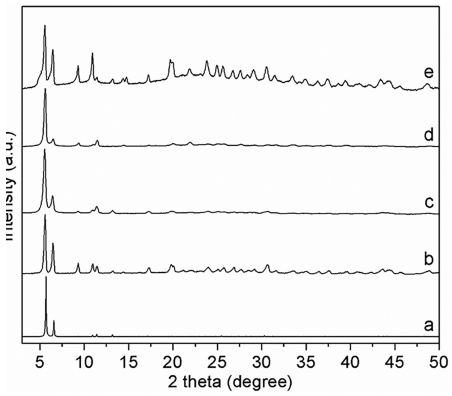

Figure 4. Powder X-ray diffraction patterns (Cu Kα, λ= 1.5418 Å): (a) Calculated from the single crystal structure of UiO-67-$(SH)_2$ (single crystal data collected at 100 K); (b) an as-made sample of UiO-67-$(SH)_2$ (the sample was covered by a DMF droplet); (c) an activated sample of UiO-67-$(SH)_2$ (Soxhlet extraction with methanol for 4 days and dried under a reduced pressure); (d) a sample of UiO-67-$(SO_3H)_2$ (the sample was covered by a DMF droplet); (e) a sample of UiO-67-$(SH)_2$ after heating in an acetonitrile solution of $PdCl_2(CH_3CN)_2$ at 70 °C for 1 day (the sample was covered by a DMF droplet).

activated sample remaining consistently sharp after long-term storage in air, e.g., for over 2 years.[34] The superior stability of the UiO-67-$(SCH_3)_4$ solid is apparently derived from the four methylthio ($-SCH_3$) groups on the TMBPD linker. These thioether groups symmetrically flank the carboxyl links to provide strong structural rigidity and steric shielding, e.g., against encroaching water molecules, around the Zr−O cluster node. By comparison, the thiol groups in UiO-67-$(SH)_2$ are smaller in both size and number, leaving the Zr−O cluster more prone to disruption by water guests. One should also note that the thiol groups can be oxidized in air to form disulfide links across the molecular struts, and thus to help strengthen the framework. The current observation, however, suggests the steric effect from dense thioether arrays of UiO-67-$(SCH_3)_4$ to be more effective in stabilizing the UiO-67-type network.

Pd Uptake and Catalytic Studies. Comparison can also be made with yet another reported sulfur-equipped MOF [i.e., UiO-68-$(SH)_2$],[6] with regards to the catalytic activity of Pd species anchored by the strongly binding thiol groups. One key feature of the UiO-68-$(SH)_2$-Pd system lies in the longer DMTBD linker and its centrally positioned thiol groups, which serve to space the S···S distances to be over 5.24 Å in the rigid framework, limiting the Pd(II) center to bond with only one single thiol unit, and leaving the coordination sphere open for catalysis (see also Figure S8). Specifically, the UiO-68-$(SH)_2$-Pd crystals with a 2.9:1 S/Pd atom ratio (reported earlier)[6] readily catalyze the Suzuki coupling (SMR) for iodo substrates with over 80% conversion rate (TON above 800) in multiple cycles without observed leaching of Pd species. The catalytic activity remains strong at lower Pd loadings of UiO-68-$(SH)_2$-Pd: For example, at 5.2:1 S/Pd atom ratio (3.74% Pd by weight), with the same temperature/reaction time (80 °C/8.0 h) and similar substrates concentrations, a conversion rate of 63% can be achieved (TON: 1563, see also Table 2), as indicated by solution NMR measurement (Figure S9).

In UiO-67-$(SH)_2$-Pd, however, the thiol groups are closer to one another, with the variable (via rotation of the phenyl units) S···S distances reaching all the way down to the bonding distance (2.0 Å); as a result, the Pd center can be more extensively bonded to the thiol groups and more severely sealed off to suppress catalytic activity. Indeed, under similar conditions, e.g., the same temperature of 80 °C and similar substrate concentrations, a polycrystalline powder sample of UiO-67-$(SH)_2$-Pd (at 4.7:1 S/Pd atom ratio) exhibits no catalytic activity for the Suzuki coupling (SMR), with no product detected even after 24 h. The catalysis, however, can be effected at a higher temperature of 100 °C, with a conversion rate of 23% and a turnover number of 104 observed (see Table 2 and Figure S10 for the associated NMR spectrum). As the pore opening (about 12 Å) of the UiO-67-$(SH)_2$ net exceeds the diameter of the substrates (about 5.8 Å), mass transport limitation, i.e., blocked diffusion, can be excluded as being key for the subdued catalytic activity of UiO-67-$(SH)_2$-Pd; instead, the more effective blocking of the Pd centers by the closely arrayed thiol groups in UiO-67-$(SH)_2$-Pd appears to offer a better rationalization.

Table 2. Catalytic Performances of Two Thiol-Tagged UiO Solids for a Suzuki−Miyaura Reaction

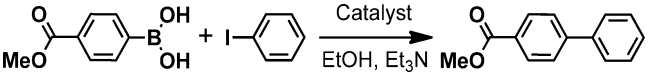

entry	catalyst	temperature (°C)	time (h)	conversion (%)	TON[a]
1	UiO-68-$(SH)_2$-Pd[b]	80	8	83.1	831
2	UiO-68-$(SH)_2$-Pd[c]	80	8	63.2	1563
3	UiO-67-$(SH)_2$-Pd[d]	80	24	0	0
4	UiO-67-$(SH)_2$-Pd	100	24	22.9	104

[a]TON (turnover number) defined as the molar ratio between the product and Pd. [b]8.68% Pd; 2.9:1 S/Pd ratio. [c]3.74% Pd; 5.2:1 S/Pd ratio. [d]6.73% Pd; 4.7:1 S/Pd ratio.

The above comparative studies (see also Table 2) on the catalytic activities of UiO-68-$(SH)_2$-Pd and UiO-67-$(SH)_2$-Pd samples illustrate how the spatial configuration of the thiol arrays can be crystal-engineered to flexibly control the bonding/coordination sphere around the Pd metal center, in order to fine-tune its chemical reactivity in a heterogeneous process afforded by the functionalized MOF matrix. Further study may reveal how controlled poisoning of the Pd centers (thus afforded by the thiol arrays) might be relevant for improving catalytic selectivity, e.g., in the hydrogenation of various organic functional groups.

Postsynthetic Oxidation. The redox-active nature of the thiol group provides a convenient entry into versatile functionalizations of the open network, including disulfide,[5] sulfenyl iodide[10,11] and sulfonic acid formation.[52] In particular, the simple and clean H_2O_2 oxidation to form sulfonic groups is of practical interest, because of the flexible configurations, e.g., dense arrays, that can be achieved for the resultant sulfonic groups and their uses for proton conductivity[13] and acid catalysis.[52] The present thiol-equipped UiO-67-type solid, i.e., Zr-DMBPD, proves especially stable to H_2O_2 oxidation, with its PXRD peaks (Figure 4, pattern d, or Figure S6, pattern c) remaining sharp and well-defined even after being treated with a strong (30% w/w) H_2O_2 solution at rt for 24 h. Analyses by FT-IR (Figure S2) and solution ^{1}H NMR (Figure S7) on the resultant solid sample indicate complete conversion of the thiol groups to the sulfonic acid ($-SO_3H$) function. Whereas the fluorescence of the pristine UiO-67-$(SH)_2$ sample is weak and hardly visible to the eye, the oxidized sample becomes distinctly fluorescent, e.g., Figures S6, and features an intense

DOI: 10.1021/acs.inorgchem.8b03000
Inorg. Chem. XXXX, XXX, XXX−XXX

emission at 443 nm in the solid-state emission spectrum (Figure S11). The turn-on fluorescence response of the UiO-67-$(SH)_2$ solid is of potential use for H_2O_2 sensing, e.g., UiO-67-$(SH)_2$ nanoparticles dispersed in physiological media may act as bioprobes for H_2O_2 monitoring.

SUMMARY

Taken together, the catalytic and stability studies on thiol-equipped porous framework of Zr-DMBPD, in comparison with two previous sulfur-functionalized isoreticular analogs [UiO-67-$(SCH_3)_4$ and UiO-68-$(SH)_2$], served to unveil the important roles of the steric and spatial configurations of the sulfur functions. To wit, higher stability to solvent loss can be effected by doubling the number of the sulfur groups around the Zr cluster node for more effective steric shielding; and closer distances among the thiol groups (affixed to the rigid host scaffold) result in stronger, chelating bonding to the Pd center, consequently sealing off its open coordination sphere and diminishing the catalytic activity. The possibility to achieve such structure−property correlation in these organic-containing solid frameworks clearly originates from the effective molecular synthetic methodology, e.g., for systematically accessing building blocks equipped with variable motifs of the sulfur functions. Molecular design and synthesis have proven crucial for in-depth studies of framework materials and will continue to do so in the future.

ASSOCIATED CONTENT

Supporting Information

The Supporting Information is available free of charge on the ACS Publications website at DOI: 10.1021/acs.inorgchem.8b03000.

TGA plot, IR and Raman spectra, solution ^{1}H NMR spectra, PXRD, and gas sorption data (PDF)

Accession Codes

CCDC 1873767 contains the supplementary crystallographic data for this paper. These data can be obtained free of charge via www.ccdc.cam.ac.uk/data_request/cif, or by emailing data_request@ccdc.cam.ac.uk, or by contacting The Cambridge Crystallographic Data Centre, 12 Union Road, Cambridge CB2 1EZ, UK; fax: +44 1223 336033.

AUTHOR INFORMATION

Corresponding Author

*E-mail: zhengtao@cityu.edu.hk.

ORCID

Matthias Zeller: 0000-0002-3305-852X

Zhengtao Xu: 0000-0002-7408-4951

Notes

The authors declare no competing financial interest.

ACKNOWLEDGMENTS

This work is supported by a GRF grant of the Research Grants Council of Hong Kong SAR (Project 11305915), Science and Technology Planning Project of Guangdong Province (2017A050506051), and Science and Technology Program of Guangzhou (201807010026).

REFERENCES

(1) Gui, B.; Meng, X.; Chen, Y.; Tian, J.; Liu, G.; Shen, C.; Zeller, M.; Yuan, D.; Wang, C. Reversible Tuning Hydroquinone/Quinone Reaction in Metal−Organic Framework: Immobilized Molecular Switches in Solid State. *Chem. Mater.* **2015**, *27*, 6426−6431.

(2) Bachman, J. E.; Kapelewski, M. T.; Reed, D. A.; Gonzalez, M. I.; Long, J. R. M2(m-dobdc) (M = Mn, Fe, Co, Ni) metal-organic frameworks as highly selective, high-capacity adsorbents for olefin/paraffin separations. *J. Am. Chem. Soc.* **2017**, *139*, 15363−15370.

(3) Levine, D. J.; Runcevski, T.; Kapelewski, M. T.; Keitz, B. K.; Oktawiec, J.; Reed, D. A.; Mason, J. A.; Jiang, H. Z. H.; Colwell, K. A.; Legendre, C. M.; FitzGerald, S. A.; Long, J. R. Olsalazine-Based Metal-Organic Frameworks as Biocompatible Platforms for H2 Adsorption and Drug Delivery. *J. Am. Chem. Soc.* **2016**, *138*, 10143−10150.

(4) He, J.; Yang, C.; Xu, Z.; Zeller, M.; Hunter, A. D.; Lin, J. Building thiol and metal-thiolate functions into coordination nets: Clues from a simple molecule. *J. Solid State Chem.* **2009**, *182*, 1821−1826.

(5) Yee, K.-K.; Reimer, N.; Liu, J.; Cheng, S.-Y.; Yiu, S.-M.; Weber, J.; Stock, N.; Xu, Z. Effective Mercury Sorption by Thiol-Laced Metal-Organic Frameworks: in Strong Acid and the Vapor Phase. *J. Am. Chem. Soc.* **2013**, *135*, 7795−7798.

(6) Gui, B.; Yee, K.-K.; Wong, Y.-L.; Yiu, S.-M.; Zeller, M.; Wang, C.; Xu, Z. Tackling poison and leach: catalysis by dangling thiol-palladium functions within a porous metal-organic solid. *Chem. Commun.* **2015**, *51*, 6917−6920.

(7) Li, M.-Q.; Wong, Y.-L.; Lum, T.-S.; Sze-Yin Leung, K.; Lam, P. K. S.; Xu, Z. Dense thiol arrays for metal-organic frameworks: boiling water stability, Hg removal beyond 2 ppb and facile crosslinking. *J. Mater. Chem. A* **2018**, *6*, 14566−14570.

(8) Pullen, S.; Fei, H.; Orthaber, A.; Cohen, S. M.; Ott, S. Enhanced photochemical hydrogen production by a molecular diiron catalyst incorporated into a metal-organic framework. *J. Am. Chem. Soc.* **2013**, *135*, 16997−17003.

(9) Liu, T.; Che, J.-X.; Hu, Y.-Z.; Dong, X.-W.; Liu, X.-Y.; Che, C.-M. Alkenyl/Thiol-Derived Metal-Organic Frameworks (MOFs) by Means of Postsynthetic Modification for Effective Mercury Adsorption. *Chem. - Eur. J.* **2014**, *20*, 14090−14095.

(10) Yee, K.-K.; Wong, Y.-L.; Xu, Z. Bio-inspired stabilization of sulfenyl iodide RS-I in a Zr(IV)-based metal-organic framework. *Dalton Trans.* **2016**, *45*, 5334−5338.

(11) Munn, A. S.; Millange, F.; Frigoli, M.; Guillou, N.; Falaise, C.; Stevenson, V.; Volkringer, C.; Loiseau, T.; Cibin, G.; Walton, R. I. Iodine sequestration by thiol-modified MIL-53(Al). *CrystEngComm* **2016**, *18*, 8108−8114.

(12) Leus, K.; Perez, J. P. H.; Folens, K.; Meledina, M.; Van Tendeloo, G.; Du Laing, G.; Van Der Voort, P. UiO-66-$(SH)_2$ as stable, selective and regenerable adsorbent for the removal of mercury from water under environmentally-relevant conditions. *Faraday Discuss.* **2017**, *201*, 145−161.

(13) Phang, W. J.; Jo, H.; Lee, W. R.; Song, J. H.; Yoo, K.; Kim, B. S.; Hong, C. S. Superprotonic Conductivity of a UiO-66 Framework Functionalized with Sulfonic Acid Groups by Facile Postsynthetic Oxidation. *Angew. Chem., Int. Ed.* **2015**, *54*, 5142−5146.

(14) Bickley, J. F.; Bonar-Law, R. P.; Femoni, C.; MacLean, E. J.; Steiner, A.; Teat, S. J. Dirhodium(II) carboxylate complexes as building blocks. Synthesis and structures of square boxes with tilted walls. *Dalton* **2000**, 4025−4027.

(15) Rosi, N. L.; Kim, J.; Eddaoudi, M.; Chen, B.; O'Keeffe, M.; Yaghi, O. M. Rod Packings and Metal-Organic Frameworks Constructed from Rod-Shaped Secondary Building Units. *J. Am. Chem. Soc.* **2005**, *127*, 1504−1518.

(16) Bloch, E. D.; Murray, L. J.; Queen, W. L.; Chavan, S.; Maximoff, S. N.; Bigi, J. P.; Krishna, R.; Peterson, V. K.; Grandjean, F.; Long, G. J.; Smit, B.; Bordiga, S.; Brown, C. M.; Long, J. R. Selective Binding of O2 over N2 in a Redox-Active Metal-Organic Framework with Open Iron(II) Coordination Sites. *J. Am. Chem. Soc.* **2011**, *133*, 14814−14822.

(17) Xiang, S.; Zhou, W.; Zhang, Z.; Green, M. A.; Liu, Y.; Chen, B. Open Metal Sites within Isostructural Metal-Organic Frameworks for Differential Recognition of Acetylene and Extraordinarily High

DOI: 10.1021/acs.inorgchem.8b03000
Inorg. Chem. XXXX, XXX, XXX−XXX

Acetylene Storage Capacity at Room Temperature. *Angew. Chem., Int. Ed.* **2010**, *49*, 4615−4618.
(18) Luo, F.; Yan, C.; Dang, L.; Krishna, R.; Zhou, W.; Wu, H.; Dong, X.; Han, Y.; Hu, T.-L.; O'Keeffe, M.; Wang, L.; Luo, M.; Lin, R.-B.; Chen, B. UTSA-74: A MOF-74 Isomer with Two Accessible Binding Sites per Metal Center for Highly Selective Gas Separation. *J. Am. Chem. Soc.* **2016**, *138*, 5678−5684.
(19) Deng, H.; Grunder, S.; Cordova, K. E.; Valente, C.; Furukawa, H.; Hmadeh, M.; Gandara, F.; Whalley, A. C.; Liu, Z.; Asahina, S.; Kazumori, H.; O'Keeffe, M.; Terasaki, O.; Stoddart, J. F.; Yaghi, O. M. Large-Pore Apertures in a Series of Metal-Organic Frameworks. *Science* **2012**, *336*, 1018−1023.
(20) Zhao, X.; Pattengale, B.; Fan, D.; Zou, Z.; Zhao, Y.; Du, J.; Huang, J.; Xu, C. Mixed-Node Metal-Organic Frameworks as Efficient Electrocatalysts for Oxygen Evolution Reaction. *ACS Energy Letters* **2018**, *3*, 2520−2526.
(21) Zhao, H.; Wang, X.; Feng, J.; Chen, Y.; Yang, X.; Gao, S.; Cao, R. Synthesis and characterization of Zn2GeO4/Mg-MOF-74 composites with enhanced photocatalytic activity for CO2 reduction. *Catal. Sci. Technol.* **2018**, *8*, 1288−1295.
(22) Kim, S. H.; Lee, Y. J.; Kim, D. H.; Lee, Y. J. Bimetallic Metal-Organic Frameworks as Efficient Cathode Catalysts for Li-O2 Batteries. *ACS Appl. Mater. Interfaces* **2018**, *10*, 660−667.
(23) Sun, L.; Hendon, C. H.; Minier, M. A.; Walsh, A.; Dincă, M. Million-Fold Electrical Conductivity Enhancement in Fe2(DEBDC) versus Mn2(DEBDC) (E = S, O). *J. Am. Chem. Soc.* **2015**, *137*, 6164−6167.
(24) Sun, L.; Miyakai, T.; Seki, S.; Dincă, M. Mn_2(2,5-disulfhydrylbenzene-1,4-dicarboxylate): A Microporous Metal-Organic Framework with Infinite (-Mn-S-)$_\infty$ Chains and High Intrinsic Charge Mobility. *J. Am. Chem. Soc.* **2013**, *135*, 8185−8188.
(25) Furukawa, H.; Gandara, F.; Zhang, Y.-B.; Jiang, J.; Queen, W. L.; Hudson, M. R.; Yaghi, O. M. Water Adsorption in Porous Metal-Organic Frameworks and Related Materials. *J. Am. Chem. Soc.* **2014**, *136*, 4369−4381.
(26) Sun, Y.; Sun, L.; Feng, D.; Zhou, H.-C. An In Situ One-Pot Synthetic Approach towards Multivariate Zirconium MOFs. *Angew. Chem., Int. Ed.* **2016**, *55*, 6471−6475.
(27) Li, Y.-A.; Yang, S.; Li, Q.-Y.; Ma, J.-P.; Zhang, S.; Dong, Y.-B. UiO-68-ol NMOF-Based Fluorescent Sensor for Selective Detection of HClO and Its Application in Bioimaging. *Inorg. Chem.* **2017**, *56*, 13241−13248.
(28) Kiang, Y.-H.; Gardner, G. B.; Lee, S.; Xu, Z.; Lobkovsky, E. B. Variable Pore Size, Variable Chemical Functionality, and an Example of Reactivity within Porous Phenylacetylene Silver Salts. *J. Am. Chem. Soc.* **1999**, *121*, 8204−8215.
(29) Eddaoudi, M.; Kim, J.; Rosi, N.; Vodak, D.; Wachter, J.; O'Keeffe, M.; Yaghi, O. M. Systematic design of pore size and functionality in isoreticular MOFs and their application in methane storage. *Science* **2002**, *295*, 469−472.
(30) Martell, J. D.; Porter-Zasada, L. B.; Forse, A. C.; Siegelman, R. L.; Gonzalez, M. I.; Oktawiec, J.; Runcevski, T.; Xu, J.; Srebro-Hooper, M.; Milner, P. J.; Colwell, K. A.; Autschbach, J.; Reimer, J. A.; Long, J. R. Enantioselective Recognition of Ammonium Carbamates in a Chiral Metal-Organic Framework. *J. Am. Chem. Soc.* **2017**, *139*, 16000−16012.
(31) McDonald, T. M.; Lee, W. R.; Mason, J. A.; Wiers, B. M.; Hong, C. S.; Long, J. R. Capture of Carbon Dioxide from Air and Flue Gas in the Alkylamine-Appended Metal-Organic Framework mmen-Mg2(dobpdc). *J. Am. Chem. Soc.* **2012**, *134*, 7056−7065.
(32) Zhou, L.-J.; Deng, W.-H.; Wang, Y.-L.; Xu, G.; Yin, S.-G.; Liu, Q.-Y. Lanthanide-Potassium Biphenyl-3,3′-disulfonyl-4,4′-dicarboxylate Frameworks: Gas Sorption, Proton Conductivity, and Luminescent Sensing of Metal Ions. *Inorg. Chem.* **2016**, *55*, 6271−6277.
(33) Cavka, J. H.; Jakobsen, S.; Olsbye, U.; Guillou, N.; Lamberti, C.; Bordiga, S.; Lillerud, K. P. A New Zirconium Inorganic Building Brick Forming Metal Organic Frameworks with Exceptional Stability. *J. Am. Chem. Soc.* **2008**, *130*, 13850−13851.
(34) Wong, Y.-L.; Yee, K.-K.; Hou, Y.-L.; Li, J.; Wang, Z.; Zeller, M.; Hunter, A. D.; Xu, Z. Single-Crystalline UiO-67-Type Porous Network Stable to Boiling Water, Solvent Loss, and Oxidation. *Inorg. Chem.* **2018**, *57*, 6198−6201.
(35) Edwards, J. D.; Pianka, M. 1346. Isomerisation of 2-butyl-4,6-dinitrophenyl thiocarbamates. *J. Chem. Soc.* **1965**, 7338.
(36) Kwart, H.; Evans, E. R. The Vapor Phase Rearrangement of Thioncarbonates and Thioncarbamates. *J. Org. Chem.* **1966**, *31*, 410−413.
(37) Newman, M. S.; Karnes, H. A. The Conversion of Phenols to Thiophenols via Dialkylthiocarbamates[1]. *J. Org. Chem.* **1966**, *31*, 3980−3984.
(38) Harvey, J. N.; Jover, J.; Lloyd-Jones, G. C.; Moseley, J. D.; Murray, P.; Renny, J. S. The Newman-Kwart Rearrangement of O-Aryl Thiocarbamates: Substantial Reduction in Reaction Temperatures through Palladium Catalysis. *Angew. Chem., Int. Ed.* **2009**, *48*, 7612−7615.
(39) Hoffmann, I.; Schatz, J. Microwave-mediated Newman-Kwart rearrangement in water. *RSC Adv.* **2016**, *6*, 80692−80699.
(40) Perkowski, A. J.; Cruz, C. L.; Nicewicz, D. A. Ambient-Temperature Newman-Kwart Rearrangement Mediated by Organic Photoredox Catalysis. *J. Am. Chem. Soc.* **2015**, *137*, 15684−15687.
(41) Wolman, Y. Protection of the thiol group. In *The Thiol Group (1974)*; John Wiley & Sons, Ltd., 2010.
(42) Harnisch, J. A.; Angelici, R. J. Gold and platinum benzenehexathiolate complexes as large templates for the synthesis of 12-coordinate polyphosphine macrocycles. *Inorg. Chim. Acta* **2000**, *300-302*, 273−279.
(43) Yip, H. K.; Schier, A.; Riede, J.; Schmidbaur, H. Benzenehexathiol as a template rim for a golden wheel: synthesis and structure of [{CSAu(PPh_3)}$_6$]. *J. Chem. Soc., Dalton Trans.* **1994**, 2333−2334.
(44) Testaferri, L.; Tiecco, M.; Tingoli, M.; Chianelli, D.; Montanucci, M. Simple Syntheses of Aryl Alkyl Thioethers and of Aromatic Thiols from Unactivated Aryl Halides and Efficient Methods for Selective Dealkylation of Aryl Alkyl Ethers and Thioethers. *Synthesis* **1983**, *1983*, 751−755.
(45) Testaferri, L.; Tingoli, M.; Tiecco, M. Reactions of polychlorobenzenes with alkanethiol anions in HMPA. A simple, high-yield synthesis of poly(alkylthio)benzenes. *J. Org. Chem.* **1980**, *45*, 4376−4380.
(46) Takagi, K.; Hayama, N.; Sasaki, K. Ni(0)-Trialkylphosphine Complexes. Efficient Homo-coupling Catalyst for Aryl, Alkenyl, and Heteroaromatic Halides. *Bull. Chem. Soc. Jpn.* **1984**, *57*, 1887−1890.
(47) Iyoda, M.; Otsuka, H.; Sato, K.; Nisato, N.; Oda, M. Homocoupling of Aryl Halides Using Nickel(II) Complex and Zinc in the Presence of Et4NI. An Efficient Method for the Synthesis of Biaryls and Bipyridines. *Bull. Chem. Soc. Jpn.* **1990**, *63*, 80−87.
(48) Takagi, K.; Hayama, N.; Inokawa, S. The in Situ-generated Nickel(0)-catalyzed Reaction of Aryl Halides with Potassium Iodide and Zinc Powder. *Bull. Chem. Soc. Jpn.* **1980**, *53*, 3691−3695.
(49) Colon, I.; Kelsey, D. R. Coupling of aryl chlorides by nickel and reducing metals. *J. Org. Chem.* **1986**, *51*, 2627−2637.
(50) Øien-Ødegaard, S.; Bouchevreau, B.; Hylland, K.; Wu, L.; Blom, R.; Grande, C.; Olsbye, U.; Tilset, M.; Lillerud, K. P. UiO-67-type Metal-Organic Frameworks with Enhanced Water Stability and Methane Adsorption Capacity. *Inorg. Chem.* **2016**, *55*, 1986−1991.
(51) Chavan, S.; Vitillo, J. G.; Gianolio, D.; Zavorotynska, O.; Civalleri, B.; Jakobsen, S.; Nilsen, M. H.; Valenzano, L.; Lamberti, C.; Lillerud, K. P.; Bordiga, S. H2storage in isostructural UiO-67 and UiO-66 MOFs. *Phys. Chem. Chem. Phys.* **2012**, *14*, 1614−1626.
(52) Yee, K.-K.; Wong, Y.-L.; Zha, M.; Adhikari, R. Y.; Tuominen, M. T.; He, J.; Xu, Z. Room-temperature acetylene hydration by a Hg(II)-laced metal-organic framework. *Chem. Commun.* **2015**, *51*, 10941−10944.

DOI: 10.1021/acs.inorgchem.8b03000
Inorg. Chem. XXXX, XXX, XXX−XXX